

Continuous-flow lithography for high-throughput microparticle synthesis

DHANANJAY DENDUKURI, DANIEL C. PREGIBON, JESSE COLLINS, T. ALAN HATTON AND PATRICK S. DOYLE*

Department of Chemical Engineering, Massachusetts Institute of Technology, Cambridge, Massachusetts 02139, USA

*e-mail: pdoyle@mit.edu

Published online: 9 April 2006; doi:10.1038/nmat1617

Precisely shaped polymeric particles and structures are widely used for applications in photonic materials¹, MEMS², biomaterials³ and self-assembly⁴. Current approaches for particle synthesis are either batch processes^{5–10} or flow-through microfluidic schemes^{11–16} that are based on two-phase systems, limiting the throughput, shape and functionality of the particles. We report a one-phase method that combines the advantages of microscope projection photolithography⁷ and microfluidics to continuously form morphologically complex or multifunctional particles down to the colloidal length scale. Exploiting the inhibition of free-radical polymerization near PDMS surfaces, we are able to repeatedly pattern and flow rows of particles in less than 0.1 s, affording a throughput of near 100 particles per second using the simplest of device designs. Polymerization was also carried out across laminar, co-flowing streams to generate Janus particles containing different chemistries, whose relative proportions could be easily tuned. This new high-throughput technique offers unprecedented control over particle size, shape and anisotropy.

Previous work on making particles in microfluidic devices^{11–15} was based on the breakoff of droplets in two-phase flows at a T-junction^{17,18} or in flow-focusing geometries¹⁹. Owing to surface-tension effects, such techniques have been restricted to generating particles that are spheres, deformations of spheres^{13,14} (rods, ellipsoids or discs) or cylinders¹⁵. Additionally, these techniques are limited to making one particle at a time, and require phase-separating chemistries (immiscible fluids) that are also surface-compatible with the microfluidic devices used.

There is a tremendous need to generate monodisperse particles with a greater diversity of shapes and with complex chemistries⁴. Such particles can serve as new building blocks in self-assembled structures, where it is known that the complexity of structures greatly increases with anisotropic interactions²⁰. These interactions can be purely steric or arise due to spatially segregated surface chemistries on a particle. Simulations show that many exotic structures can be created with anisotropic interactions, but a technology to synthesize a comprehensive particle library is lacking⁴. Furthermore, microparticles can act as surfactants, and their assembly depends subtly on their morphology²¹. The rheology of particle suspensions is also very sensitive to particle shape, and

is important in the design of bullet-resistant fabrics²², paints and consumer products.

Complex particles are also needed in the emerging field of barcoded-particle technologies²³. Existing techniques typically add new functional groups one-by-one²⁴. A one-step synthesis is highly desired. Challenges also exist in aligning particles before detection, and custom shapes may facilitate this.

Using a new technique, we are able to overcome the above limitations to continuously synthesize a variety of different shapes using several different oligomers and make bifunctional Janus particles. The method is straightforward to implement using a standard fluorescence microscope, and can easily be extended to create particles that have more than two distinct coded (for example, chemically, fluorescently, magnetically) regions in a one-step synthesis.

In a representative experiment, an acrylate oligomer stream (typically poly(ethylene glycol) diacrylate) containing a photosensitive initiator was passed through a rectangular, all-PDMS microfluidic device as shown in Fig. 1a. Particle arrays of mask-defined shapes (see squares in Fig. 1b) were formed by exposing the flowing oligomer to controlled pulses of ultraviolet (UV) light using an inverted microscope and collected in the device reservoir (Fig. 2). Rapid polymerization kinetics permitted the particles to form quickly (<0.1 s), and oxygen-aided inhibition near the PDMS surfaces allowed for particle flow within the unpolymerized oligomer stream (see Supplementary Information, Movie S1). This serendipitous ability of the particles to flow is because molecular oxygen diffusing through the PDMS surfaces reacts with initiator species to form chain-terminating peroxide radicals²⁵, leaving a non-polymerized lubricating layer (see Supplementary Information, Section S2) near the PDMS walls (inset of Fig. 1a). The phenomenon of oxygen inhibition at the PDMS walls is applicable to any free-radical polymerization, rendering our approach suitable for a broad range of polymer chemistries.

The shape of the particles in the x - y plane (Fig. 1b) is determined by the shape of the feature used on the transparency mask (Fig. 1a), whereas the z -plane projection (shown in Fig. 1c) is dependent on the height of the channel used and the thickness of the oxygen inhibition layer. Using our microscope projection setup,

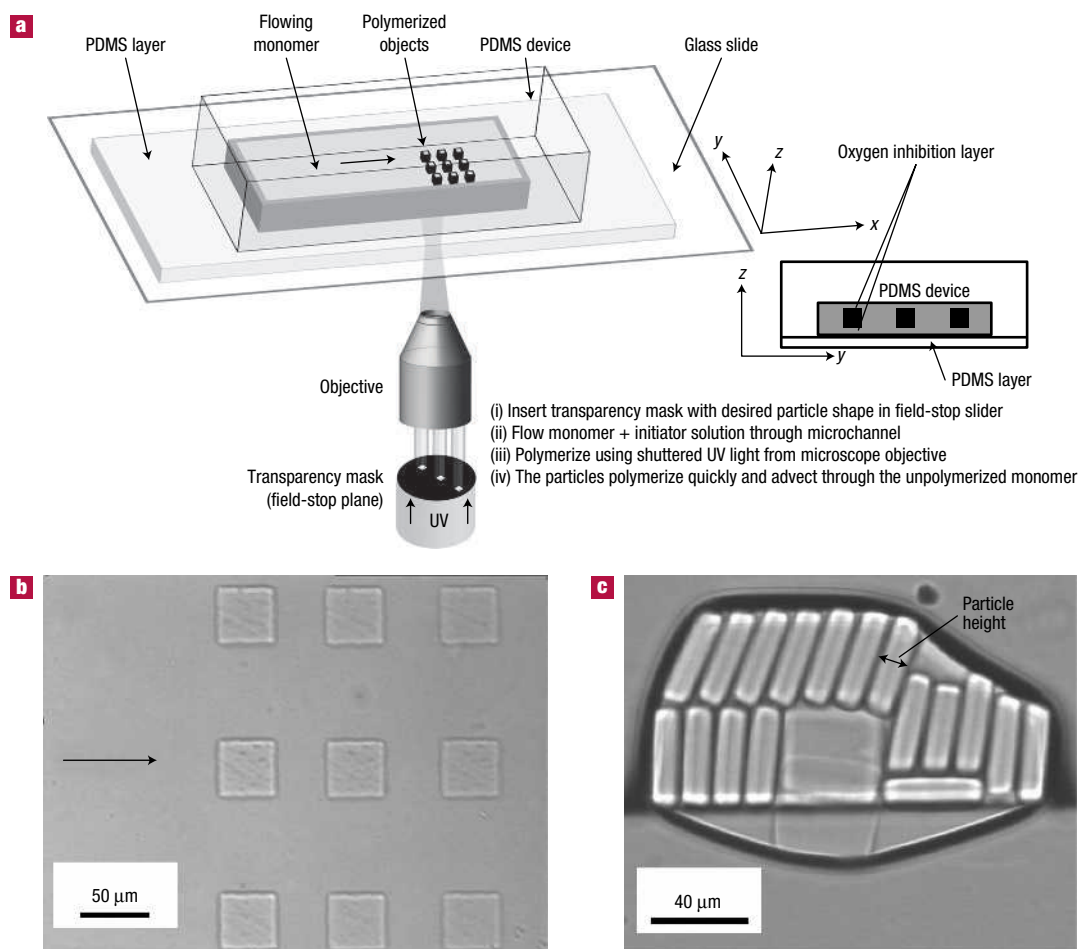


Figure 1 **Experimental setup.** **a**, Schematic depicting the experimental setup used in the study. A mask containing the desired features is inserted in the field-stop plane of the microscope. The monomer stream flows through the all-PDMS device in the direction of the horizontal arrow. Particles are polymerized, by a mask-defined UV light beam emanating from the objective, and then advect within the unpolymerized monomer stream. The side-view of the polymerized particles can be seen in the inset shown on the right. Also shown is the unpolymerized oxygen inhibition layer that allows the particles to flow easily after being formed. **b**, A brightfield microscopy image (x - y plane) of an array of cuboids moving through the unpolymerized monomer. **c**, A cross-sectional view of the cuboids seen in **b** upon collection in a droplet that has turned most particles on their sides.

the transparency feature sizes were reduced by a factor dictated by the objective used, ranging from 7.8 times using a $\times 20$ objective to 39 times using a $\times 100$ objective. For example, using the $\times 20$ objective, a 350- μm -square mask feature was used to synthesize cuboids (rectangular parallelepiped objects) that had 45- μm sides ($350\ \mu\text{m}/7.8 = 45\ \mu\text{m}$) in the x - y plane (Fig. 1b). The height of the particles was equal to the height of the channel minus the thickness of the inhibition layers (see Supplementary Information, Section S2). Cuboids with a height of 15 μm (Fig. 1c) were synthesized in a 20- μm -high channel because of the 2.5- μm -thick oxygen inhibition layer at both the top and bottom walls of the device. By designing masks with varied features and selecting channels of differing heights, we synthesized particles of several distinctive shapes, sizes and aspect ratios (Figs 2, 3).

We have synthesized various polygonal shapes such as triangles, squares and hexagons (Fig. 3a-c); colloidal entities (Fig. 3d); high-aspect-ratio objects such as posts with circular, triangular and square cross-sections (Fig. 3e,f); and non-symmetric or curved objects (Fig. 3g-i). All of the particles showed good fidelity to the original mask features and had straight sidewalls.

The fundamental limitations of a projection photolithography technique, such as ours, are mainly governed by the optical resolution and the depth of field of the microscope objective used (see Supplementary Information, Section S3). The resolution of an objective is the smallest distinguishable feature that can be discerned, and the depth of field is the length over which the beam of light emanating from the objective can be considered to have a constant diameter. In our case, the resolution limits the size of the smallest particle that can be made, whereas the depth of field restricts the length over which the sidewalls will be straight. Better resolution comes at the cost of decreased depth of field. Additionally, practical constraints on particle synthesis are imposed by finite polymerization times and the minimum feature size currently printable on a transparency mask ($\sim 10\ \mu\text{m}$).

The exposure time required to polymerize particles was inversely proportional to both the height of the channels used and the size of the transparency mask feature (see Supplementary Information, Section S4); particles required longer polymerization times when either of these two parameters was decreased. The oxygen inhibition layer thickness is independent of channel height,

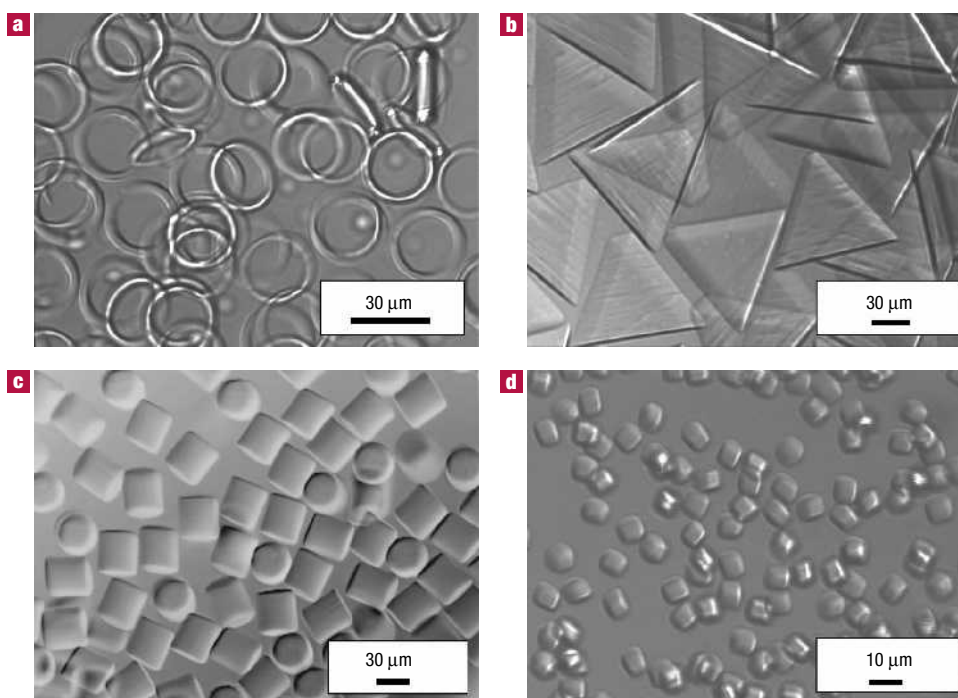


Figure 2 Differential interference contrast images of collections of particles. Particles were generated in a high-throughput fashion and collected in a reservoir. **a**, Rings formed using a 9.6- μm -high channel and the $\times 20$ objective. **b**, Triangles formed in a 38- μm -high channel using a triangular mask and the $\times 20$ objective. **c**, Cylinders synthesized using circular masks in 38- μm -high channels using the $\times 20$ objective. **d**, Colloidal cuboids synthesized using a square mask and the $\times 20$ objective in a 9.6- μm -high channel. All of the particles were synthesized using exposure times obtained from the data shown in Section S4 of Supplementary Information.

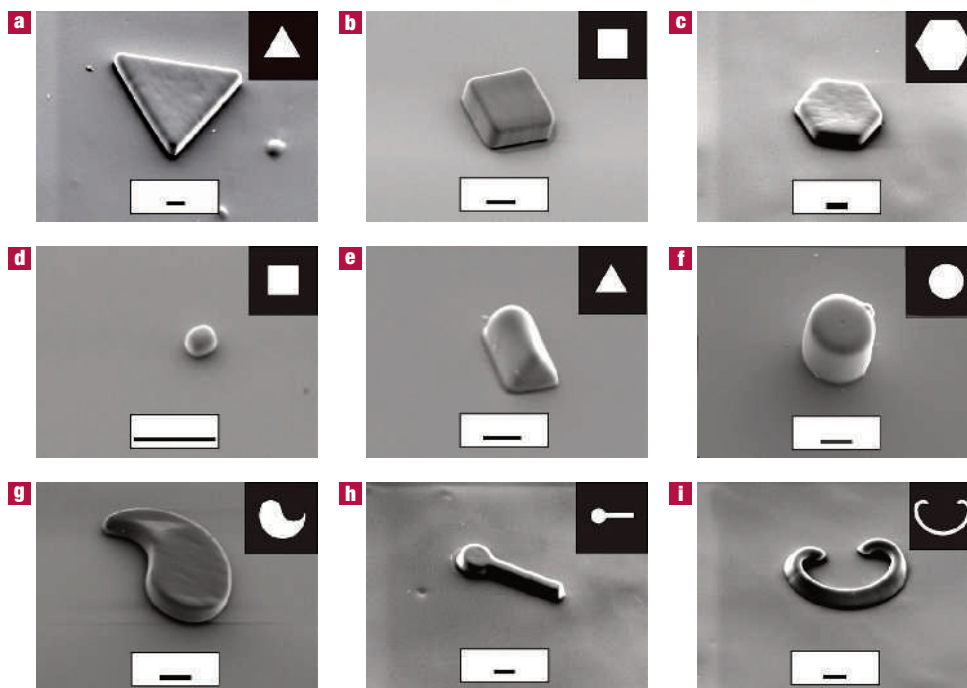


Figure 3 Scanning electron microscope images of particles. Microparticles formed using a $\times 20$ objective (except **d**, which was formed using a $\times 40$ objective) were washed before being observed using SEM. The scale bar in all of the figures is 10 μm . **a–c**, Flat polygonal structures that were formed in a 20- μm -high channel. **d**, A colloidal cuboid that was formed in a 9.6- μm -high channel. **e, f**, High-aspect-ratio structures with different cross-sections that were formed in a 38- μm -high channel. **g–i**, Curved particles that were all formed in a 20- μm -high channel. The inset in the figure shows the transparency mask feature that was used to make the corresponding particle. All of the particles were synthesized using exposure times obtained from the data in Section S4 of Supplementary Information.

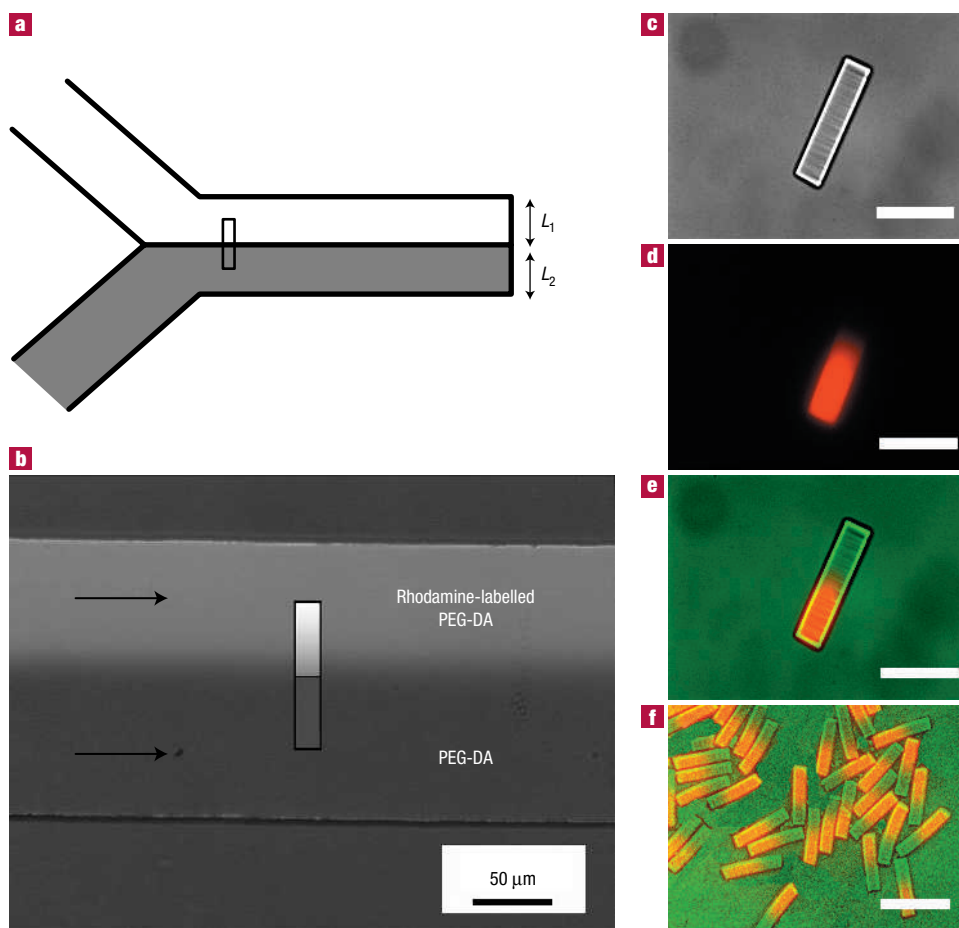


Figure 4 Synthesis of Janus particles. **a**, A schematic diagram showing the synthesis of Janus (two-faced) particles. The widths of the streams, L_1 and L_2 , can be altered by changing the flow rates of the streams. **b**, Two streams containing PEG-DA (grey) and PEG-DA with rhodamine-labelled cross linker (white) are co-flowed through a channel. A schematic representing the formation of a bar-shaped particle $130\ \mu\text{m}$ in length and $20\ \mu\text{m}$ width is overlaid on the picture. Diffusion-limited mixing seen in laminar flow is exploited to ensure the streams flow distinctly. **c**, DIC image of a Janus particle. **d**, Fluorescence microscopy image of the particle in **c**. The rhodamine-labelled portion is seen in red. **e**, An overlaid image of the entire particle showing both the fluorescently labelled (orange) and the non-labelled (green) sections. The scalebar in figures **c–e** is $50\ \mu\text{m}$. **f**, Multiple Janus particles with the fluorescent portion shown in orange. The scalebar is $100\ \mu\text{m}$.

leading to more-pronounced effects in low-height channels, where the layer occupies a larger fraction of the channel height (see Supplementary Information, Section S2). Smaller transparency feature sizes require increased polymerization doses as a result of diffraction-induced limitations in the internal microscope optics (see Supplementary Information, Section S5). Longer polymerization times lead to constraints on the maximum velocity of the oligomer stream, to avoid shape deformation of the particles (see Supplementary Information, Section S6). Although we have only generated particles greater than $3\ \mu\text{m}$ using continuous flow, preliminary experiments showed that we could synthesize even smaller objects ($\sim 1\ \mu\text{m}$) in a stop-polymerize-flow mode. In addition to controlling particle size and shape, our approach allows for the selection of various particle chemistries. The oligomer streams used in this process can incorporate diverse functional moieties to synthesize particles that are field-responsive²⁶, pH- and temperature-responsive²⁷, or protein-loaded⁸ for applications in self-assembly, rheology, biosensing and drug delivery.

Entities with multiple chemistries^{27–29} are proving to be important in sorting and targeting applications²³ or in self-assembly studies⁴. Using our technique, particles with

two or more functionalities may be easily and controllably synthesized. Exploiting the diffusion-limited mixing seen in laminar flow (Fig. 4a,b), we synthesized bifunctional Janus particles (Fig. 4c–e) by polymerizing rectangular particles across the interface of co-flowing and rhodamine-labelled oligomer streams. By controlling the location of the interface using the flow rates of the streams or the location of the projected light by moving the microscope stage, we can synthesize particles that contain variable proportions of different chemistries. By simply flowing multiple, concurrent, laminar streams through a microfluidic device and polymerizing particles across these streams, our approach may be used to generate particles with several adjacent chemistries. The ability to tune the proportion of so many chemistries allows for great flexibility in the design of barcoded particles.

We have demonstrated a photolithography-based microfluidic technique that can be used to continuously synthesize polymeric particles of varied complex shapes and multiple chemistries. The advantage over traditional lithography techniques^{6,7} is the continuous nature of the process, permitting the high-throughput ($400,000\ \text{particles h}^{-1}$) generation of polymeric particles. In a next-generation device, we could increase the area of the light

source and parallelize the technology to achieve much higher throughput. The morphology and the chemistry of the particles can be independently chosen to form large numbers of uniquely shaped, functionalized particles for applications including drug delivery, biosensors, microactuators and fundamental studies on self-assembly and rheology. Greater control of particle morphology could potentially be achieved using grey-scale photomasks, multiphoton illumination or multiple-beam lithography³⁰. This technique presents an opportunity for the high-throughput synthesis of morphologically or chemically unique particles for various applications.

METHODS

MATERIALS

All of the particles shown in this work were made using 5% (v/v) solutions of Darocur 1173 (Sigma Aldrich) initiator in poly(ethylene glycol)(400) diacrylate (PEG-DA, Polysciences). The viscosity of the PEG-DA is reported by the supplier to be 57 cP at 25 °C. We also made particles composed of trimethylpropane triacrylate, 1,6-hexanediol diacrylate and tri(propylene glycol) diacrylate (all from Polysciences). All of these materials belong to the class of multifunctional acrylate molecules that are known to be highly reactive and form tightly cross linked networks upon radical-induced polymerization. The method should work for other radical-induced polymerizations because they are, in general, inhibited by oxygen²⁵. Solutions, 0.005 wt%, of the fluorescent methacryloxyethyl thiocarbonyl rhodamine B (Polysciences) in PEG-DA were used to fluorescently label the polymer.

MICROFLUIDIC DEVICES

Devices were fabricated by pouring polydimethylsiloxane (PDMS, Sylgard 184, Dow Corning) on a silicon wafer containing positive-relief channels patterned in SU-8 photoresist (Microchem). The devices were rectangular channels of varying widths (200, 600 or 1,000 µm) and heights (9.6, 20 or 38 µm). These devices were placed on glass slides spin-coated with PDMS to ensure that the oligomer was only exposed to the PDMS surfaces. The devices were mounted on an inverted microscope (Axiovert 200, Zeiss), and the formation of the microparticles was visualized using a charge-coupled-device camera (KPM1A, Hitachi). Images were captured and processed using NIH Image software.

PHOTOPOLYMERIZATION SETUP

Photomasks were designed in AUTOCAD 2005 and printed using a high-resolution printer at CAD Art Services (Poway, California). The mask was then inserted into the field-stop of the microscope. A 100 W HBO mercury lamp served as the source of UV light. A filter set that allowed wide UV excitation (11000v2: UV, Chroma) was used to select light of the desired wavelength and a VS25 shutter system (Uniblitz) driven by a computer-controlled VMM-D1 shutter driver provided specified pulses of UV light. Oligomer solutions were driven through the microfluidic device using a KDS 100 syringe pump (KD Scientific).

PARTICLE RECOVERY AND CHARACTERIZATION

The particles were collected, washed and then re-suspended three times in ethanol to dissolve the unpolymerized PEG-DA. They were then washed three times in water, and finally suspended in water. The particle size distribution and extent of polymerization were quantified using standard methods (see Supplementary Information, Section S7).

Received 26 October 2005; accepted 22 February 2006; published 9 April 2006.

References

- Lu, Y., Yin, Y. & Xia, Y. Three-dimensional photonic crystals with non-spherical colloids as building blocks. *Adv. Mater.* **13**, 415–420 (2001).
- Beebe, D. J. *et al.* Functional hydrogel structures for autonomous flow control inside microfluidic channels. *Nature* **404**, 588–590 (2000).
- Langer, R. & Tirrell, D. A. Designing materials for biology and medicine. *Nature* **428**, 487–492 (2004).
- Glotzer, S. C. Some assembly required. *Science* **306**, 419–420 (2004).
- Urban, D. & Takamura, K. (eds) *Polymer Dispersions and Their Industrial Applications* (Wiley-VCH, Weinheim, Germany, 2002).
- Brown, A. B. D., Smith, C. G. & Rennie, A. R. Fabricating colloidal particles with photolithography and their interactions at an air-water interface. *Phys. Rev. E* **62**, 951–960.
- Love, J. C., Wolfe, D. B., Jacobs, H. O. & Whitesides, G. M. Microscope projection photolithography for rapid prototyping of masters with micron-scale features for use in soft lithography. *Langmuir* **17**, 6005–6012 (2001).
- Rezvin, A. *et al.* Fabrication of poly(ethylene glycol) hydrogel microstructures using photolithography. *Langmuir* **17**, 5440–5447 (2001).
- Jiang, P., Bertone, J. F. & Colvin, V. L. A lost-wax approach to monodisperse colloids and their crystals. *Science* **291**, 453–457 (2001).
- Rolland, J. P. *et al.* Direct fabrication and harvesting of monodisperse, shape-specific nanobiomaterials. *J. Am. Chem. Soc.* **127**, 10096–10100 (2005).
- Sugiyura, S., Nakajima, M., Tong, J., Nabetani, H. & Seki, M. Preparation of monodispersed solid lipid microspheres using a microchannel emulsification technique. *J. Colloid Interface Sci.* **227**, 95–103 (2000).
- Nisisako, T., Torii, T. & Higuchi, T. Novel microreactors for functional polymer beads. *Chem. Eng. J.* **101**, 23–29 (2004).
- Dendukuri, D., Tsoi, K., Hatton, T. A. & Doyle, P. S. Controlled synthesis of nonspherical microparticles using microfluidics. *Langmuir* **21**, 2113–2116 (2005).
- Xu, S. *et al.* Generation of monodisperse particles by using microfluidics: control over size, shape and composition. *Angew. Chem. Int. Edn* **44**, 724–728 (2005).
- Jeong, W. *et al.* Hydrodynamic microfabrication via 'on the fly' photopolymerization of microscale fibers and tubes. *Lab Chip* **4**, 576–580 (2004).
- Subramaniam, A. B., Abkarian, M. & Stone, H. A. Controlled assembly of jammed colloidal shells on fluid droplets. *Nature Mater.* **4**, 553–556 (2005).
- Nisisako, T., Torii, T. & Higuchi, T. Droplet formation in a microchannel network. *Lab Chip* **2**, 24–26 (2002).
- Thorsen, T., Roberts, R. W., Arnold, F. H. & Quake, S. R. Dynamic pattern formation in a vesicle-generating microfluidic device. *Phys. Rev. Lett.* **86**, 4163–4166 (2001).
- Anna, S. L., Bontoux, N. & Stone, H. A. Formation of dispersions using 'flow focusing' in microchannels. *Appl. Phys. Lett.* **82**, 364–366 (2003).
- Glotzer, S. C., Solomon, M. J. & Kotov, N. A. Self-assembly: From nanoscale to microscale colloids. *AIChE J.* **50**, 2978–2985 (2004).
- Binks, B. P. Particles as surfactants—similarities and differences. *Curr. Opin. Colloid Interface Sci.* **7**, 21–41 (2002).
- Lee, Y. S., Wetzel, E. D. & Wagner, N. J. The ballistic impact characteristics of kevlar woven fabrics impregnated with a colloidal shear thickening fluid. *J. Mater. Sci.* **38**, 2825–2833 (2003).
- Finkel, N. H., Lou, X., Wang, C. & He, L. Barcoding the microworld. *Anal. Chem.* **76**, 352A–359A (2004).
- Nicewarner-Pea, S. R. *et al.* Submicrometer metallic barcodes. *Science* **294**, 137–141 (2001).
- Decker, C. & Jenkins, A. D. Kinetic approach of O₂ inhibition in ultraviolet- and laser-induced polymerizations. *Macromolecules* **18**, 1241–1244 (1985).
- Zrinyi, M. Intelligent polymer gels controlled by magnetic fields. *Colloid Polym. Sci.* **278**, 98–103 (2000).
- Kim, S. *et al.* Hydrodynamic fabrication of polymeric barcoded strips as components for parallel bio-analysis and programmable microactuation. *Lab Chip* **5**, 1168–1172 (2005).
- Roh, K.-H., Martin, D. C. & Lahann, J. Biphasic Janus particles with nanoscale anisotropy. *Nature Mater.* **4**, 759–763 (2005).
- Fialkowski, M., Bitner, A. & Grzybowski, B. A. Self-assembly of polymeric microspheres of complex internal structures. *Nature Mater.* **4**, 93–97 (2005).
- Ullal, C. K. *et al.* Photonic crystals through holographic lithography: Simple cubic, diamond-like, and gyroid-like structures. *Appl. Phys. Lett.* **84**, 5434–5436 (2004).

Acknowledgements

We gratefully acknowledge the support of NSF NIRT Grant No. CTS-0304128 for this project. We thank Y. Hu for assistance with fluorescence microscopy, as well as K. Krogman and J. Lutkenhaus for assistance with FTIR measurements.

Correspondence and requests for materials should be addressed to P.S.D.

Supplementary Information accompanies this paper on www.nature.com/naturematerials.

Competing financial interests

The authors declare that they have no competing financial interests.

Reprints and permission information is available online at <http://npg.nature.com/reprintsandpermissions/>